Hindawi Publishing Corporation
Journal of Nanomaterials
Volume 2014, Article ID 428390, 9 pages
http://dx.doi.org/10.1155/2014/428390

Research Article

Resistance Fluctuations in GaAs Nanowire Grids

Ivan Marasović,[1] Željka Milanović,[2] and Tihomir Betti[1]

[1] *Faculty of Electrical Engineering, Mechanical Engineering and Naval Architecture, University of Split, Ruđera Boškovića 32, 21000 Split, Croatia*
[2] *Faculty of Engineering, University of Rijeka, Vukovarska 58, 51000 Rijeka, Croatia*

Correspondence should be addressed to Ivan Marasović; ivan.marasovic@fesb.hr

Received 5 March 2014; Accepted 2 May 2014; Published 9 July 2014

Academic Editor: Tianyou Zhai

Copyright © 2014 Ivan Marasović et al. This is an open access article distributed under the Creative Commons Attribution License, which permits unrestricted use, distribution, and reproduction in any medium, provided the original work is properly cited.

We present a numerical study on resistance fluctuations in a series of nanowire-based grids. Each grid is made of GaAs nanowires arranged in parallel with metallic contacts crossing all nanowires perpendicularly. Electrical properties of GaAs nanowires known from previous experimental research are used as input parameters in the simulation procedure. Due to the nonhomogeneous doping, the resistivity changes along nanowire. Allowing two possible nanowire orientations ("upwards" or "downwards"), the resulting grid is partially disordered in vertical direction which causes resistance fluctuations. The system is modeled using a two-dimensional random resistor network. Transfer-matrix computation algorithm is used to calculate the total network resistance. It is found that probability density function (PDF) of resistance fluctuations for a series of nanowire grids changes from Gaussian behavior towards the Bramwell-Holdsworth-Pinton distribution when both nanowire orientations are equally represented in the grid.

1. Introduction

Modern electronics industry tends to move from traditional silicon technology towards novel materials with improved characteristics. Special interest is given to nanostructure materials, since in the quantum confinement regime their optical and electrical properties are determined by their size. This fact opens a possible route for production of electronic devices which are faster, have better sensitivity, and are more energy efficient. A group of extensively studied nanostructures for applications in electronic devices are semiconductor nanowires (NW). The basic nanowire application in electronics is for field effect transistors [1–4], but there are also numerous papers reporting applications in optoelectronics, for example, for lasers [5–7] or solar cells [8–12]. Nanowires also hold great potential in building sensors, since they have large surface-to-volume ratio while their diameter is in the size range of species being sensed [13]. Usually, sensing is realized by monitoring the change in nanowire conductance upon exposure to sensed species. It was also suggested that a nanowire can be used as a basic light-sensing unit in a more complex structure like nanowire grid [14]. A theoretical study has been made using random resistor network methodology as the basis for modeling such partially disordered systems. Here, we extend previous study by in-depth analysis of resistance fluctuations in nanowire grids. These fluctuations, caused by different nanowire orientations, are simulated for a large set of nanowire sensing grids. Behavior and the shape of probability density function (PDF) of resistance fluctuations are investigated and explained in terms of nanowire orientation distribution. Electrical properties of GaAs nanowires obtained experimentally [15, 16] are used as the input parameters for simulations.

2. GaAs Nanowire Grid

Nanowires are solid rod-like structures with diameter smaller than 100 nm with typical length-to-width ratio of 1000 or more. There are several key issues related to their successful implementation: growth control, doping, processing, characterization, and application possibilities. All these issues have been widely studied, mostly for single nanowire samples. Recently, we have proposed a light-sensing device consisting of many nanowires, arranged in series/parallel to form a grid with metallic contacts [14]. The idea is based on the significant

change of a nanowire resistance upon light exposure. Here we refer to the results of electrical characterization of GaAs nanowires done by Fontcuberta group [15, 16], with typical I-V curves shown in Figure 1.

Nanowire growth and characterization procedures are described in detail elsewhere [9, 15–18]. Two and four-point probe measurements were performed on 15 nanowire samples. Each nanowire was produced with multiple, equally spaced contacts. In this way, the spatial dependence of the resistivity was determined and the results of a representative nanowire are taken for our model. It was found that the resistivity decreases along nanowire from the top to the bottom as a result of nonhomogeneous doping. In other words, not all parts of the nanowire will have the same light sensitivity and it will depend on nanowire doping profile. Therefore, we introduced coarse distinction between "active" and "passive" parts of the nanowire, in Figure 2. The fraction of active segments (FoS) is then defined as the ratio between the length of active segments L_{as} and the total length of a nanowire L_{tot}:

$$\text{FoS} = \frac{L_{as}}{L_{tot}} \cdot 100\%. \quad (1)$$

It was shown by simulations [14] that FoS is a critical parameter for light sensitivity of the nanowire grid. The results of electrical and optical characterization [15, 16] suggest that reasonable assumption for studied p-doped GaAs nanowires would be FoS = 20%, meaning active segments would be those whose resistance per length is within 30% from the maximum value. However, we have taken FoS as the input parameter for the model to allow different doping profiles. Resistance of each nanowire segment is different and depends on the level of doping, number of contacts, and distance from the top of the nanowire. The measured spatial dependence of resistivity is fitted by a second-order polynomial thus allowing the calculation of the resistivity of an arbitrary nanowire segment. Contact resistance also changes along nanowire so the same procedure is repeated to find the adequate mathematical model (fifth-order polynomial function). Detailed discussion on the nanowire segment resistance can be found in [14].

One of the biggest challenges in fabricating nanowire-based electronic devices like sensors, actuators, and memories is controlled assembly of nanowires into functional structures. This means the control of each nanowire position and orientation is required, as well as control of the distance between nanowires (pitch). A number of successful techniques for regular nanowire arrangement are reported in the literature [19–25], proving that high degree of regularity is achievable in parallel nanowire arrays. In reality, there will always be slight deviation from perfectly parallel alignment. If angular orientations are neglected, the real geometry is reduced to two basic orientations. Realistic and ideal nanowire grids are shown in Figure 3, where deviations in case of realistic nanowire grid are more emphasized for illustration. In case of ideal geometry, the grid would consist of identical nanowires aligned in parallel and of metallic contacts crossing all nanowires perpendicularly. Then, only possible "disorder" stems from different nanowire orientations,

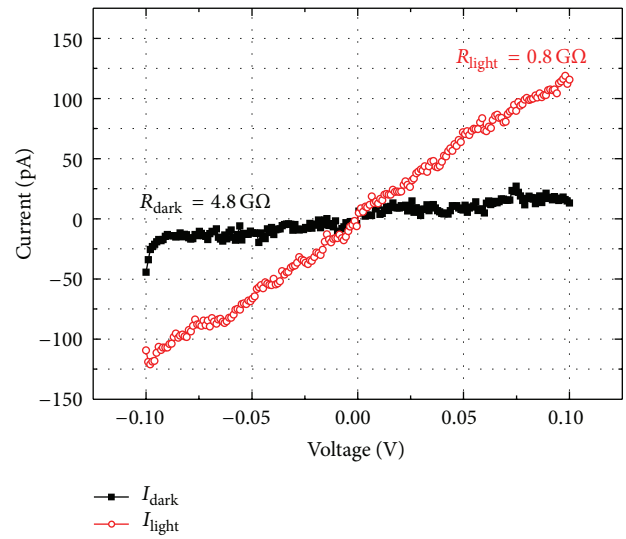

Figure 1: Single undoped GaAs nanowire I-V curves in the dark (black squares) and under microscope light (red circles) (reprinted with permission from [14]).

since the nanowire base has lower resistance than the tip. It is important to point out that each nanowire in the structure can be directed upwards (with tip at uppermost contact) or downwards (with tip at lowermost contact). However, if we suppose that every nanowire can take any of two allowed directions with certain probability, this probability would play important role in determining electrical properties of entire nanowire grid. Furthermore, increasing the number of nanowires in the grid reduces the chance of producing two identical devices. Hence, it is necessary to study a larger set of samples in order to extract information about orientations distribution. As the first step towards quality control of produced nanowire grids, we used computer simulations to analyze relevant macroscopic quantities.

3. Modeling a Nanowire Grid

As already mentioned, we considered ideal nanowire grid, as illustrated in Figure 3. Neglecting the thickness of nanowires and metallic contacts, the structure is basically a two-dimensional system. Under the assumption that all nanowires in the network are identical, as well as all metallic contacts, the complete system can be considered as a random resistor network (RRN) made of two types of resistors: nanowire segments are resistors with higher resistance, while metallic contacts represent resistors of small resistance. The nanowire and metallic contact resistance are determined from mathematical expressions obtained by fitting to the measured data for GaAs nanowires.

We have considered rectangular network with dimensions $N \times L$, where N represents number of nanowire (vertical) segments and L is the number of metallic (horizontal) segments. If outermost contacts are treated as terminals made of highly conductive material, terminal resistance can be neglected and total number of resistors N_{tot} is determined by

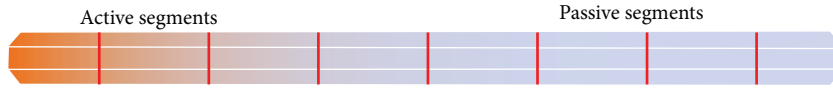

Figure 2: Active and passive segments of nanowire.

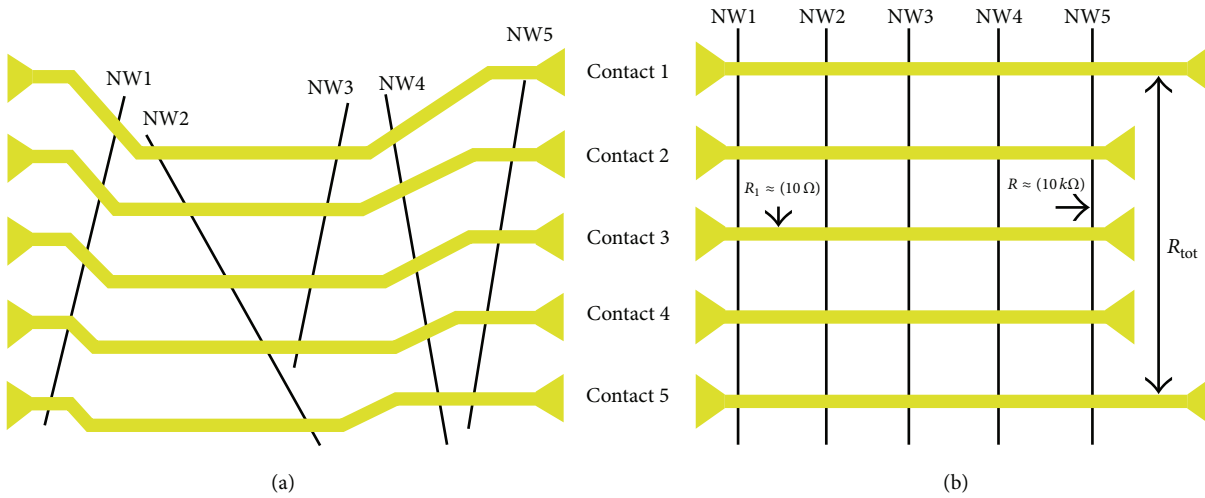

Figure 3: Nanowire grids with realistic geometry (a) and ideal geometry (b) used in simulation.

$2N \times L$. Total resistance R_{tot} and total resistance fluctuations δR_{tot} as the most important parameters which describe electrical properties of the system are determined. Analysis included networks of different sizes, containing arbitrary number of metallic contacts with variable intercontact distance. To describe proposed nanowire grid, we have modified general RRN model introducing several constraints.

(i) Resistance fluctuations of vertical and horizontal elements (resistors) are negligible.

(ii) The resistance of outermost contacts (terminals) is negligible.

(iii) Nanowires are considered as vertical elements only.

(iv) Inner metallic contacts are considered as horizontal elements only.

Regarding constant resistance of horizontal metallic segments, vertical segments alternations cause total resistance fluctuations. In this case, nanowire orientations determine vertical segments alternations and should be crucial parameter for total resistance analysis.

3.1. Method: Transfer-Matrix Formulation. The main parameter describing electrical properties of nanowire grid is the total resistance, which can be calculated using several different methods or by direct application of Kirchhoff's laws. For large networks we employed transfer-matrix formulation which is based on consecutive enlargement of the network in one direction by adding horizontal and vertical segments shown in Figure 4. Network is expanded by increasing its length to $L + 1$, that is, by adding one column of horizontal and vertical segments. These segments are represented by their respective vectors h_i and v_i containing resistances of ith horizontal and of ith vertical segments. Further, $V[N \times N]$ and $H[N \times N]$ are the tridiagonal matrices obtained from v_i and h_i elements by using rules defined in [26]. Expansion of nanowire grid changes conditions in the network resulting in the new transfer matrix A_{L+1} that can be calculated using recursive relation [26]:

$$A_{L+1} = V + A_L\left(I + HA_L\right)^{-1}, \tag{2}$$

where I is unit matrix of size $N \times N$. Vertical resistors correspond to resistance of nanowire segments and horizontal resistors represent the resistance of metallic segments and the contact resistance between metal and nanowire. At each step, the transfer matrix for resulting network is determined.

Finally, the conductance of complete network is defined as first element of inverse transfer matrix [26]. Then, total resistance R_{tot} is given as

$$R_{tot} = \left[A_L^{-1}(1,1)\right]^{-1}. \tag{3}$$

Inverted transfer matrix is symmetrical and contains other information that could be useful for network analysis. The first line and the first column of the inverted transfer matrix are identical and contain values corresponding to node potentials in the last vertical branch in case unit current flows through the grid.

The main problem in determination of total resistance of nanowire grid is calculation of inverse transfer matrix contained in the second part of (2). When calculation is based on iterative method, like in our case, the matrix condition number grows in each calculation step. If the condition number is too large, transfer matrix becomes ill-conditioned

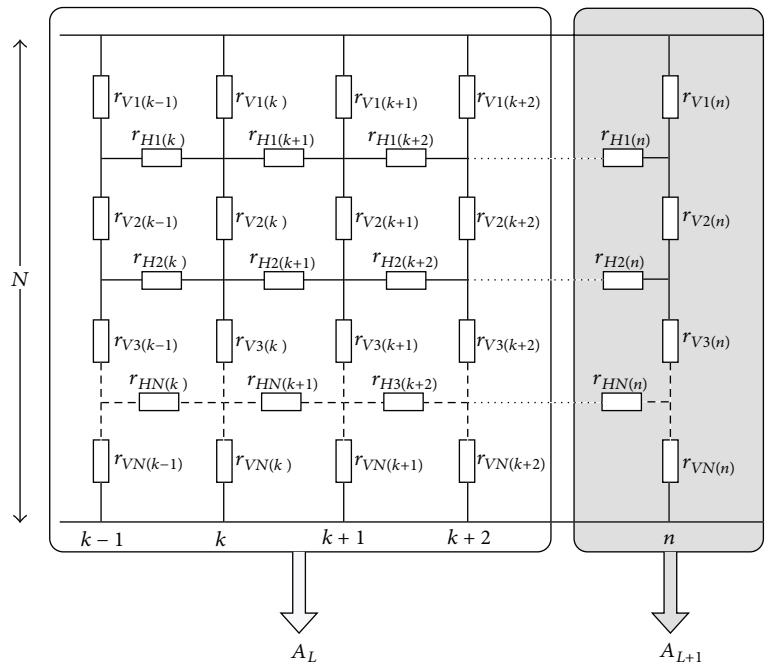

Figure 4: Expansion of nanowire grid and transfer matrix formulation for RRN model (reprinted with permission from [14]).

and eventually singular. For singular matrix direct calculation of the inverse is impossible and pseudo-inverse is used. In this step, accuracy is reduced and obtained results may be strongly affected by transfer-matrix condition number. Hence, it is desirable that the ratio between the resistance of horizontal and vertical segments is as small as possible. This also means that, for the sake of stability and accuracy of proposed calculation method, it is necessary to consider nanowire segments as vertical and metallic segments as horizontal elements of the grid to avoid or reduce accumulation of error. The pseudo-inverse can be expressed from the singular value decomposition (SVD) as follows:

$$A_L^{-1} = [V]\,[S]^{-1}[U]^T, \tag{4}$$

where U, V are both orthogonal matrices and S is a diagonal matrix containing the (positive) singular values of A_L on its diagonal.

4. Results and Discussion

Using a model of partially ordered resistor network and applying transfer-matrix method, we have calculated fluctuations of the total resistance in the series of nanowire grids. Distribution of fluctuations is the key parameter in evaluating entire series of the produced light-sensing devices. Calculations are done for constant network sizes, fractions of active segments, and dark/light nanowire resistance ratios while orientation of nanowires is varied. The sensitivity of the grid resistance to the number of nanowires and their orientations is calculated and discussed.

Analysis of the total resistance dependency on the grid size, (defined with number of nanowires L and number of metallic contacts N) is reported in the previous study [14]. However, if all nanowires were identical, then contact resistance and resistance of metallic contacts would have no influence on total grid resistance. In such case, the resistance is defined by parallel connection of nanowires, meaning it can be calculated as

$$R_{\text{tot}} = \sum_{i=1}^{N} \frac{R_{vi}}{L}, \tag{5}$$

where R_{vi} is the resistance of ith (out of N) nanowire segment. Number of contacts and intercontact distance should be optimized according to the practical application (e.g., for solar cells it is necessary to ensure efficient collection of photo-generated carriers). According to average nanowire length and contact width from previous experimental work, in this paper we have estimated the number of contacts to be $N = 20$, unless stated otherwise.

In order to evaluate how these fluctuations change with grid size, we have analyzed grids comprising 50, 100, and 500 nanowires. For each grid size, 1000 different grids with random nanowire orientations were generated and total grid resistance was calculated. This simulation step represents manufacturing process where sensing grid with different nanowire orientations is produced. Hence, further simulations are focused on the series of sensing grids with different nanowire orientations in order to evaluate the manufacturing process.

The results presented in Figure 5 show that larger number of nanowires not only reduces total grid resistance, but also reduces the magnitude of relative resistance fluctuations. From this analysis, one can conclude that larger number of nanowires enhances overall stability of the grid and reduces the sensitivity to nanowire orientation. Hence, to achieve

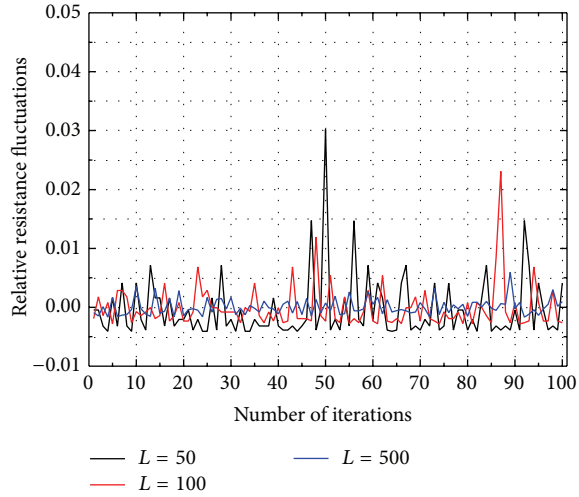

FIGURE 5: Relative resistance fluctuations of total network resistance for grid length $L = 10$, 50, and 100.

resistance stability and better insight into resistance fluctuations caused by nanowire orientation, larger horizontal dimension $L = 500$ (number of nanowires) of the sensing grid is chosen.

In all previous cases, it was assumed that the orientation of nanowires follows the uniform distribution. If one orientation is preferred, total resistance and relative resistance fluctuations will change, as shown in Figure 6. It should be noted that the lowest total resistance is obtained with uniform distribution of nanowire orientations, and the resistance increases as one orientation under production becomes more dominant. All results shown in Figure 6 are obtained as a light response while the same behavior and trends are also found in dark resistance response of the nanowire sensing grid. For comparison, in Figure 7 relative variance of the resistance fluctuations for dark and light is reported. Relative variance shows quasilinear dependence on the nanowire orientation and increase for high order in the grid. When increasing the grid order, relative variance shows saturation and finally decreases. Under the light, the amplitude of relative variance is approximately three times higher than the amplitude obtained in the dark for entire range of the nanowire orientations. Distribution of nanowire orientations almost has no influence on power spectral density which again follows flicker noise-like behavior. Therefore, power spectral density cannot be used as an indicator of orientation distribution (disorder) in nanowire sensing grid and further research will be focused to probability density function (PDF) of resistance fluctuations.

In Figure 8 simulation results as PDF of resistance fluctuations are given and qualitatively compared with theoretical distributions, Gaussian and Bramwell-Holdsworth-Pinton (BHP) distribution [27]. It is evident that for one dominant orientation PDFs show Gaussian-like behavior for both light and dark responses of sensing grid. Reducing the difference between probabilities of possible nanowire orientations increases the probability of negative fluctuations increases (distribution tail) and simulated PDF converges towards the theoretical BHP distribution. However, when both nanowire orientations in the grid are represented with equal probability (50 : 50) distribution tail shows higher oscillations.

The same behavior is also detected in other complex physical systems (percolation systems, granular media, forest fires, and quantum dots ensembles) both in critical and steady-state close turbulent regimes [27]. Although origin of distribution tail in complex systems is unknown, our simulations confirm strong correlation between nanowire orientations and the shape of PDF curve. From qualitative analysis of simulation results and comparison with theoretical distributions it is evident that probability density function describes fluctuations of total resistance as macroscopic quantity both in ordered and disordered states and provides insight into the nanowire sensing grid structure. Comparing dark and light PDFs given in Figure 9, it is evident that negative fluctuations for sensing grid under light (Figure 9(b)) are higher than the resistance fluctuations in the dark (Figure 9(a)). On the other hand, positive fluctuations under light follow BHP distribution more closely, including certain offsets regarding the saddle of the BHP distribution. In case of equal nanowire orientation probability similar oscillatory behavior is found both for dark and light conditions. Under the light slightly higher amplitude of the oscillations is observed.

Results reported in Figure 8 show that distribution tail oscillates when nanowire grid converges towards equal nanowire orientation probability and this effect is more significant under light condition. For better insight into distribution tail generated by enhancement of negative fluctuations, cumulative distribution function (CDF) is computed and reported in Figure 9. For this purpose CDF is shown only for negative fluctuations with limit value to −1. When one nanowire orientation dominates, distribution tail closely follows the shape of normal distribution both for dark and light conditions. On the other side, in disordered sensing grids CDF of the distribution tail under light shows larger divergence from the BHP distribution and exists for more negative fluctuations than CDF in the dark. In order to determine deviation simulation CDF from normal distribution, chi-square test of independence for interval of x from −5 to −1 is performed. Significant difference was observed for 85 : 15 distributions of nanowire orientations both for dark and light conditions (d.f. 68, chi = 92.23). In accordance to previous conclusion, probability density function is fitted to BHP distribution for nanowire orientation distributions in the range of 80 : 20 to 50 : 50. BHP distribution is defined for the entire range of normalized fluctuations according to [27]

$$\Pi(x) = K\left(e^{y-e^{y}}\right)^{a}; \qquad y = b(x-s), \tag{6}$$

where K, b, and s are distribution parameters found analytically.

By using nonlinear least squares method (implemented through LM algorithm) for each PDF defined with nanowire orientation, BHP distribution is fitted and corresponding parameters are calculated. Considering the distribution tail

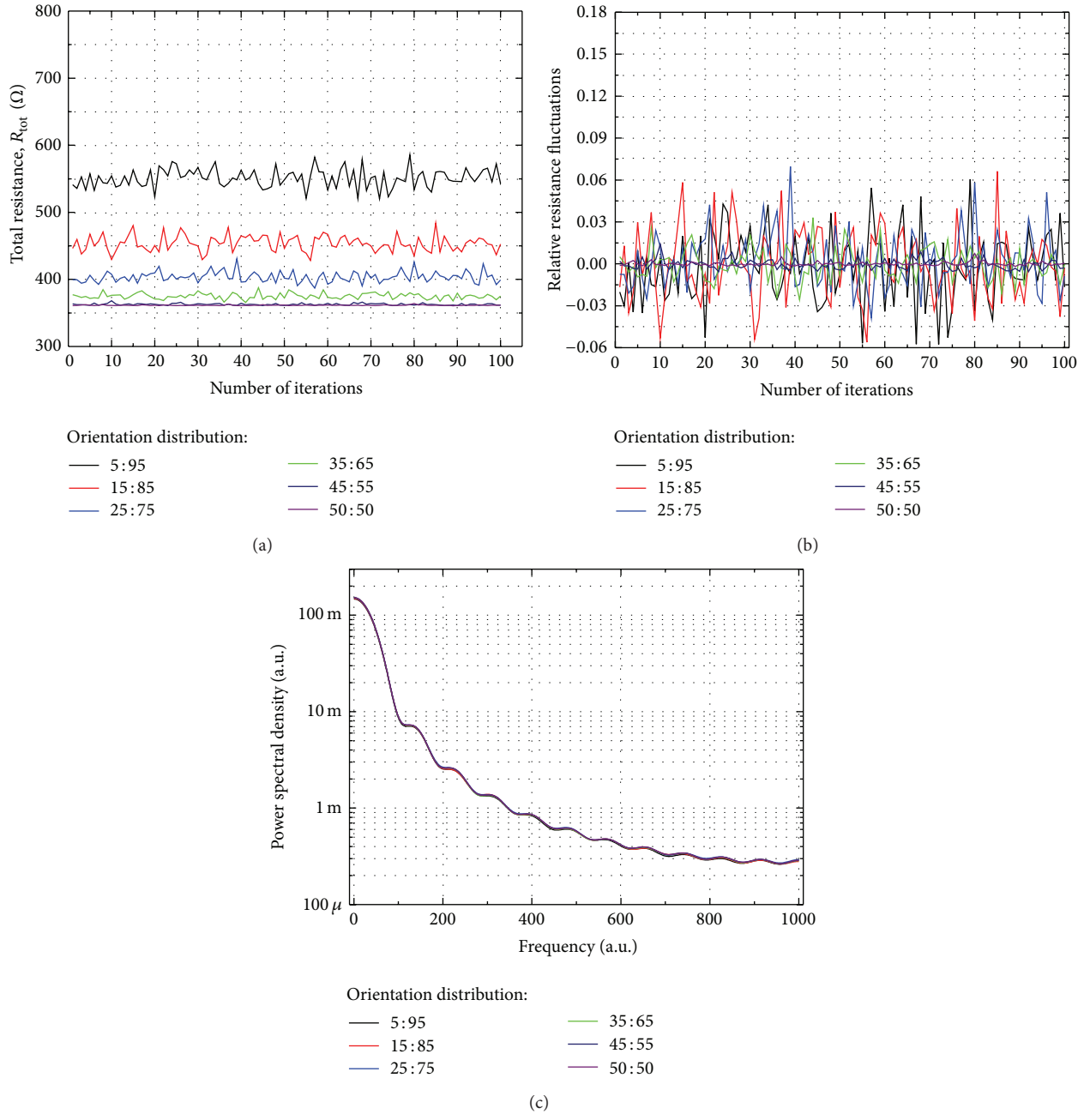

Figure 6: Total grid resistance for various distributions of nanowire orientations (a). Relative resistance ratio is given in (b). Power spectral density (c) is very similar in all considered cases. In all cases, nanowire grid $L = 500$.

defined by negative fluctuations ($x \ll x_{\text{saddle}}$), asymptotic values of PDF can be expressed as

$$\Pi(x) \propto |x| \exp\left(-\frac{\pi}{2} b x\right). \tag{7}$$

Distribution tail is primarily defined by nanowires orientation distribution as shown in Figure 10 and can be quantified by BHP distribution parameter b according to (7). In this sense, functional dependency of parameter b and nanowire orientation distribution probability p is computed and the results are shown in Figure 10. Parameter b is higher for equilibrium probability, exponentially decays, and finally saturates in highly ordered sensing grids. It is also obvious that parameter b shows higher values and stronger exponential dependence in the dark than under light. That means slightly increased distribution tail in the dark as supported by comparing PDFs shown in Figures 9(a) and 9(b). Simulation results are fitted to the exponential functions as follows:

$$b_{\text{dark}}(x) = k_1 e^{k_2 (p - k_3)^{k_4}}, \tag{8a}$$

$$b_{\text{light}}(x) = x h_1 e^{h_2 (p - h_3)^{h_4}}, \tag{8b}$$

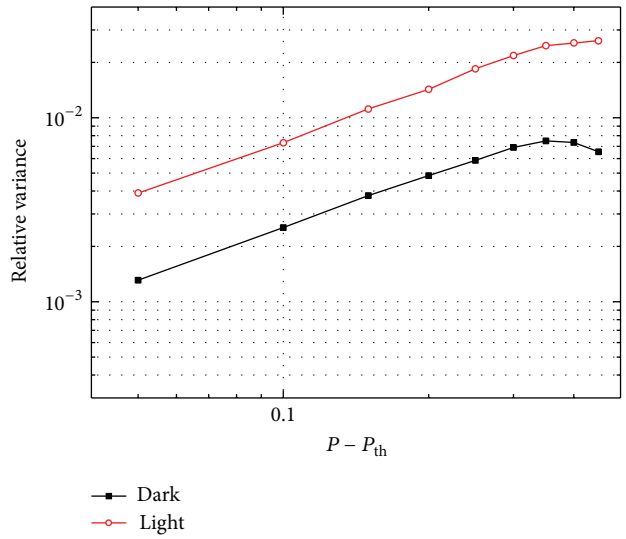

FIGURE 7: Relative variance of resistance fluctuations as a function of the nanowire orientations where P_{th} represents probability threshold ($P_{th} = 0.5$).

where k_1–k_4 and h_1–h_4 are coefficients of the fitted function. Simulated results and fitted functions for probability range of interest are shown in Figure 10.

Based on the knowledge of the parameter b and using (8a)-(8b) or graphical method (using Figure 10) the probability of nanowire orientations distribution can be derived. If parameter b is not derived by fitting simulation results to BHP distribution then it can be extracted from asymptotic of PDF using (7) as follows:

$$b = -\frac{2}{\pi}\frac{1}{|x|}\ln\left(\frac{10^{nx+c}}{|x|}\right), \tag{9}$$

where n and c represent slope and intercept of the asymptotic line, respectively.

With described approach, based on the analysis of resistance fluctuations PDF, it is possible to easily determine nanowire orientations distribution in the set of different nanowire grids. Nanowire orientations determine the position of active part of the grid which is more light-sensitive. Hence, the shape of PDF curve of nanowire grid resistivity and its deviation from the Gaussian distribution and convergence towards BHP could be the initial indicator of the nanowire orientation disorder (probability) in a series of the manufactured samples.

5. Conclusion and Outlook

We have studied resistance fluctuations in a set of nanowire sensing grids with different nanowire orientation distributions. A random resistor network model has been used to describe the grid and the total resistance is calculated using transfer-matrix algorithm. It is shown that total grid resistance and resistance fluctuations strongly depend on

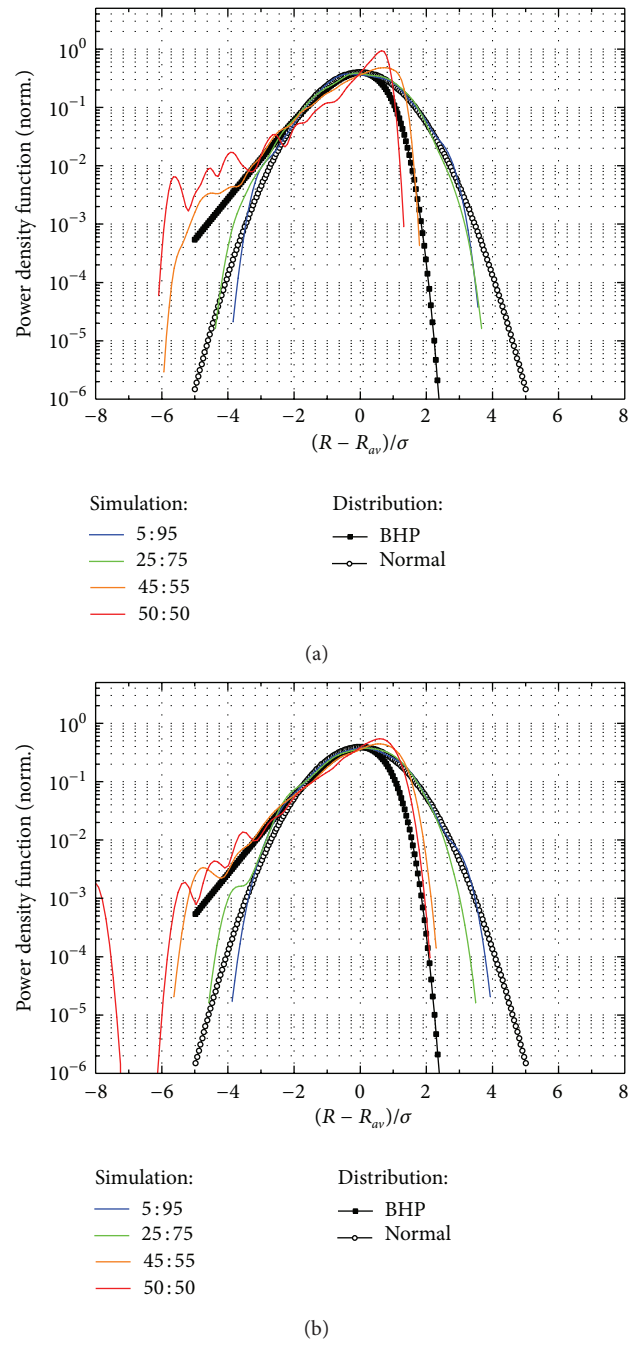

FIGURE 8: Normalized PDF for various distributions of the nanowire orientations under (a) dark and (b) light conditions.

distribution of nanowire orientations. In case when one orientation is dominant, both total resistance and relative resistance fluctuations are the highest and the probability density function of total resistance fluctuations exhibits Gaussian behavior. As the difference between orientation probabilities is reduced, fluctuation distribution diverges from the Gaussianity towards the theoretical Bramwell-Holdsworth-Pinton (BHP) distribution. We have then proposed a simple method, how to extract the information on nanowire orientation distributions from the shape of probability density function

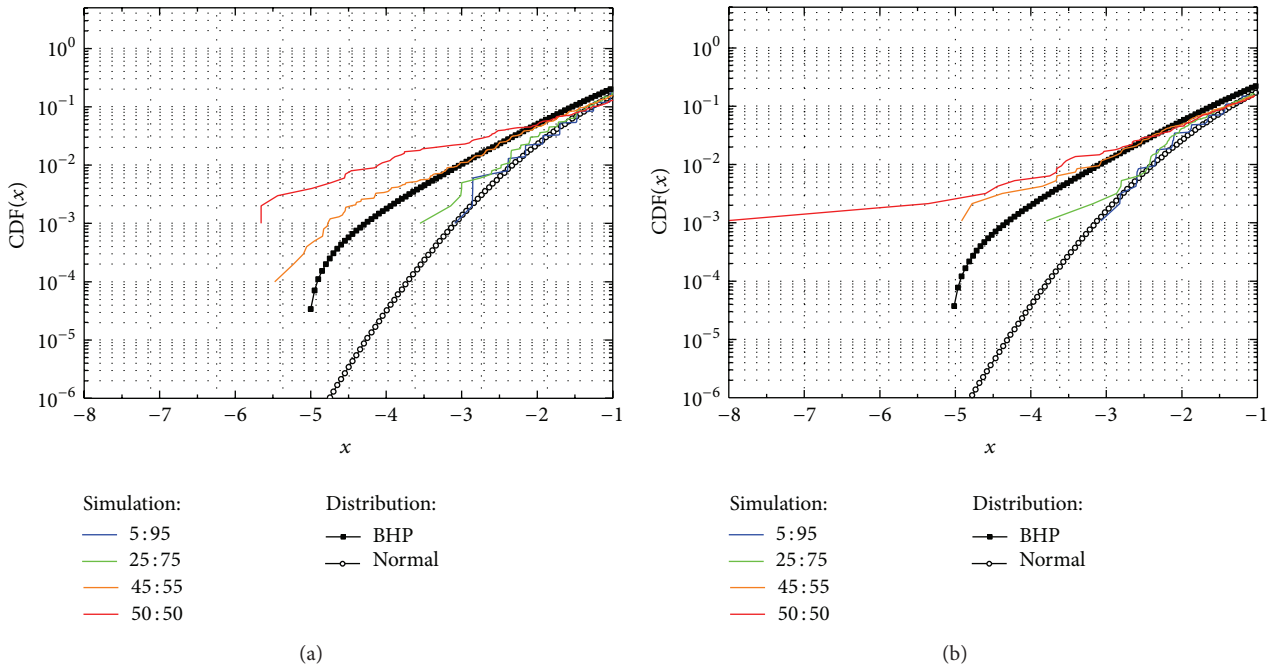

Figure 9: Cumulative distribution function (CDF) for various distributions of the nanowire orientations under (a) dark and (b) light conditions. In this report x limited to −1 represents normalized resistance fluctuations $(R - R_{av})/\sigma$.

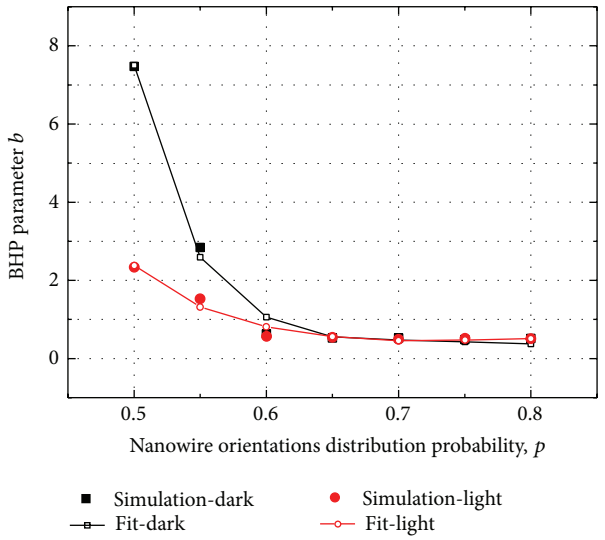

Figure 10: BHP parameter b as a function of the nanowire orientation distribution.

of resistance fluctuations. This means that measuring macroscopic quantity (total resistance) can give some insights about the structure of the studied system which might be very useful, especially for devices based on nanostructures where other structural characterization techniques are more time consuming.

Conflict of Interests

The authors declare that there is no conflict of interests regarding the publication of this paper.

Acknowledgments

The authors would like to thank Ivan Zulim for fruitful discussions and experimental support. This work was financed by Croatian Ministry of Science, Education and Sports.

References

[1] D. Vashaee, A. Shakouri, J. Goldberger, T. Kuykendall, P. Pauzauskie, and P. Yang, "Electrostatics of nanowire transistors with triangular cross sections," *Journal of Applied Physics*, vol. 99, no. 5, Article ID 054310, 2006.

[2] J. Xiang, W. Lu, Y. Hu, Y. Wu, H. Yan, and C. M. Lieber, "Ge/Si nanowire heterostructures as high-performance field-effect transistors," *Nature*, vol. 441, no. 7092, pp. 489–493, 2006.

[3] J. Goldberger, A. I. Hochbaum, R. Fan, and P. Yang, "Silicon vertically integrated nanowire field effect transistors," *Nano Letters*, vol. 6, no. 5, pp. 973–977, 2006.

[4] J. Goldberger, D. J. Sirbuly, M. Law, and P. Yang, "ZnO nanowire transistors," *Journal of Physical Chemistry B*, vol. 109, no. 1, pp. 9–14, 2005.

[5] A. B. Greytak, C. J. Barrelet, Y. Li, and C. M. Lieber, "Semiconductor nanowire laser and nanowire waveguide electro-optic modulators," *Applied Physics Letters*, vol. 87, no. 15, Article ID 151103, pp. 1–3, 2005.

[6] J. C. Johnson, H.-J. Choi, K. P. Knutsen, R. D. Schaller, P. Yang, and R. J. Saykally, "Single gallium nitride nanowire lasers," *Nature Materials*, vol. 1, no. 2, pp. 106–110, 2002.

[7] X. Duan, Y. Huang, R. Agarwal, and C. M. Lieber, "Single-nanowire elecctrically driven lasers," *Nature*, vol. 421, no. 6920, pp. 241–245, 2003.

[8] B. Tian, X. Zheng, T. J. Kempa et al., "Coaxial silicon nanowires as solar cells and nanoelectronic power sources," *Nature*, vol. 449, no. 7164, pp. 885–889, 2007.

[9] C. Colombo, M. Heiβ, M. Grätzel, and A. Fontcuberta i Morral, "Gallium arsenide *p-i-n* radial structures for photovoltaic applications," *Applied Physics Letters*, vol. 94, Article ID 173108, 2009.

[10] M. D. Kelzenberg, D. B. Turner-Evans, B. M. Kayes et al., "Photovoltaic measurements in single-nanowire silicon solar cells," *Nano Letters*, vol. 8, no. 2, pp. 710–714, 2008.

[11] E. C. Garnett and P. Yang, "Silicon nanowire radial p-n junction solar cells," *Journal of the American Chemical Society*, vol. 130, no. 29, pp. 9224–9225, 2008.

[12] T. Stelzner, M. Pietsch, G. Andrä, F. Falk, E. Ose, and S. Christiansen, "Silicon nanowire-based solar cells," *Nanotechnology*, vol. 19, no. 29, Article ID 295203, 2008.

[13] F. Patolsky and C. M. Lieber, "Nanowire nanosensors," *Materials Today*, vol. 8, no. 4, pp. 20–28, 2005.

[14] I. Marasovic, T. Garma, and T. Betti, "Modelling a nanowire grid for light-sensing applications," *Journal of Physics D: Applied Physics*, vol. 45, no. 21, Article ID 215103, 2012.

[15] T. Garma, "Semiconductor nanowires and their field-effect devices," 2011.

[16] J. Dufouleur, C. Colombo, T. Garma et al., "P-Doping mechanisms in catalyst-free gallium arsenide nanowires," *Nano Letters*, vol. 10, no. 5, pp. 1734–1740, 2010.

[17] C. Colombo, D. Spirkoska, M. Frimmer, G. Abstreiter, and A. Fontcuberta I Morral, "Ga-assisted catalyst-free growth mechanism of GaAs nanowires by molecular beam epitaxy," *Physical Review B*, vol. 77, no. 15, Article ID 155326, 2008.

[18] A. Fontcuberta I Morral, K. Maslov, C. Colombo, G. Abstreiter, J. Arbiol, and J. R. Morant, "Nucleation mechanism of gallium-assisted molecular beam epitaxy growth of gallium arsenide nanowires," *Applied Physics Letters*, vol. 92, Article ID 149903, 2008.

[19] A. I. Hochbaum, R. Fan, R. He, and P. Yang, "Controlled growth of Si nanowire arrays for device integration," *Nano Letters*, vol. 5, no. 3, pp. 457–460, 2005.

[20] Y. Huang, X. Duan, Q. Wei, and C. M. Lieber, "Directed assembly of one-dimensional nanostructures into functional networks," *Science*, vol. 291, no. 5504, pp. 630–633, 2001.

[21] P. A. Smith, C. D. Nordquist, T. N. Jackson et al., "Electric-field assisted assembly and alignment of metallic nanowires," *Applied Physics Letters*, vol. 77, no. 9, pp. 1399–1401, 2000.

[22] D. Whang, S. Jin, Y. Wu, and C. M. Lieber, "Large-scale hierarchical organization of nanowire arrays for integrated nanosystems," *Nano Letters*, vol. 3, no. 9, pp. 1255–1259, 2003.

[23] X. Liu, Y. Z. Long, L. Liao, X. Duan, and Z. Fan, "Large-scale integration of semiconductor nanowires for high-performance flexible electronics," *ACS Nano*, vol. 6, no. 3, pp. 1888–1900, 2012.

[24] N. A. Melosh, A. Boukai, F. Diana et al., "Ultrahigh-density nanowire lattices and circuits," *Science*, vol. 300, no. 5616, pp. 112–115, 2003.

[25] Z. Fan, J. C. Ho, Z. A. Jacobson et al., "Wafer-scale assembly of highly ordered semiconductor nanowire arrays by contact printing," *Nano Letters*, vol. 8, no. 1, pp. 20–25, 2008.

[26] B. Derrida and J. Vannimenus, "A transfer-matrix approach to random resistor networks," *Journal of Physics A: Mathematical and General*, vol. 15, no. 10, pp. L557–L564, 1982.

[27] S. T. Bramwell, P. C. W. Holdsworth, and J.-F. Pinton, "Universality of rare fluctuations in turbulence and critical phenomena," *Nature*, vol. 396, no. 6711, pp. 552–554, 1998.

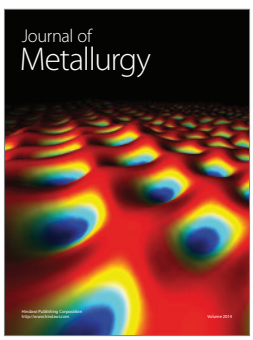

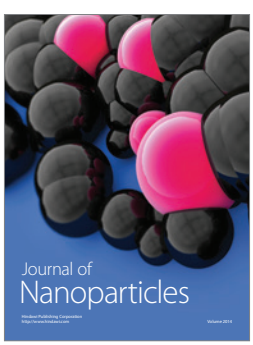

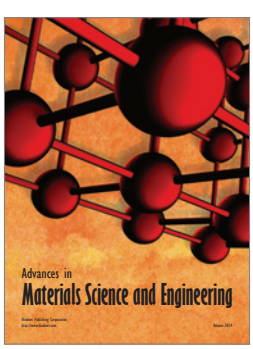

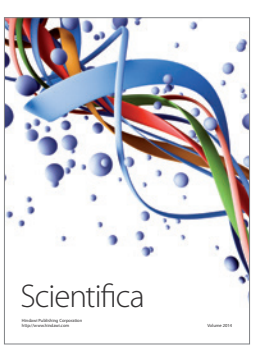

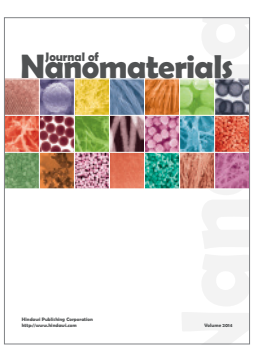

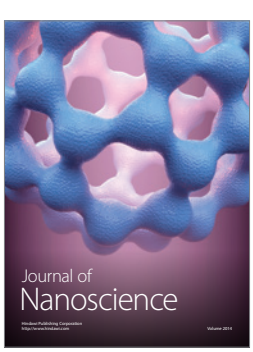

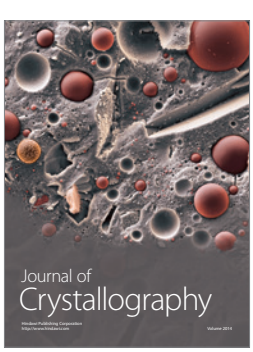

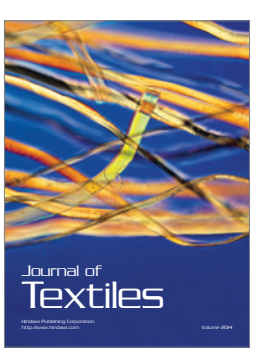

Hindawi

Submit your manuscripts at
http://www.hindawi.com